

# The LISA benchtop simulator at the University of Florida

**Rachel J Cruz, James I Thorpe, Alix Preston, Rodrigo Delgadillo, Michael Hartman, Shawn Mitryk, Aaron Worley, Gabriel Boothe, Sridhar R Guntaka, Sergei Klimenko, David B Tanner and Guido Mueller**

Department of Physics, University of Florida, PO Box 118440, Gainesville, FL 32611-8440, USA

E-mail: [rachel@phys.ufl.edu](mailto:rachel@phys.ufl.edu) and [mueller@phys.ufl.edu](mailto:mueller@phys.ufl.edu)

Received 1 April 2006, in final form 17 July 2006

Published 15 September 2006

Online at [stacks.iop.org/CQG/23/S751](http://stacks.iop.org/CQG/23/S751)

## Abstract

At the University of Florida, we are developing an experimental Laser Interferometer Space Antenna (LISA) simulator. The foundation for the simulator is a pair of cavity-stabilized lasers that provide realistic, LISA-like phase noise. The light travel time over the five million kilometres between spacecraft is recreated in the lab by use of an electronic phase delay technique. Initial tests will focus on phasemeter implementation, time delay interferometry (TDI) and arm-locking. In this paper we present the frequency stabilization results, results from an electronic arm-locking experiment, software phasemeter performance and results from a first optical experiment to test the TDI concept. In the future, the benchtop simulator will be extended to test several other aspects of LISA interferometry such as clock noise and Doppler shifts of the signals. The eventual long-term use of the LISA simulator will be to provide realistic data streams, including all the noise components, into which model gravitational wave signals can be injected. This will make the simulator a useful testbed for data analysis research groups.

PACS numbers: 42.60.–v, 95.75.Kk, 95.85.Sz

(Some figures in this article are in colour only in the electronic version)

## 1. Introduction: LISA

The Laser Interferometer Space Antenna (LISA) is a joint NASA–ESA mission to detect gravitational waves in the frequency range of  $3 \times 10^{-5}$  to 1 Hz from objects such as galactic binaries, super-massive black hole mergers and extreme mass ratio inspirals. LISA consists of three spacecraft in a triangular formation with five million kilometre arms. Each of the identical spacecraft has two optical benches, which are each oriented at one of the far spacecraft. Each

optical bench houses a proof mass, which the spacecraft shields from outside forces so that they may act as freely falling test particles of the gravitational field. Interferometry is used to monitor the change in distance between all proof masses to detect a passing gravitational wave.

The main challenge for LISA interferometry is that the laser phase noise is several orders of magnitude larger than the expected signal from a gravitational wave. There are three approaches to reduce the noise to the required sensitivity: pre-stabilization [1], arm-locking [2] and time delay interferometry (TDI) [3]. Pre-stabilization uses an external reference, such as an optical cavity or a molecular transition, to stabilize the frequency of the laser. Arm-locking uses the LISA arm as a stable reference to further suppress the frequency noise, and TDI algorithms will be used post-process to cancel the remaining noise. At the University of Florida (UF), we are currently developing a ground-based simulator to evaluate implementation strategies for LISA interferometry. Our initial efforts focus on pre-stabilization, arm-locking and first-generation TDI. In this paper we present our frequency stabilization results, describe the electronic phase delay technique, give results of an electronic arm-locking experiment, give our software phasemeter performance and discuss an initial optical experiment using the benchtop simulator to verify the TDI concept. By developing the simulator, we will also produce LISA-like data streams which will be available for data analysis tests.

## 2. The benchtop simulator

### 2.1. Laser frequency stabilization

LISA will use frequency-stabilized lasers or lasers that are phase-locked to a frequency-stabilized laser. The current LISA baseline calls for an optical reference cavity made from a low expansion glass. At UF, we assembled two reference cavities from Schott's Zerodur glass with optically contacted mirrors. The cavities are enclosed by five cylindrical layers of thermal insulation, each made of gold-plated, stainless-steel sheets. The concentric cylinders are separated by Macor spacers and the entire structure is located inside a large vacuum tank. It is expected that the temperature stability of the environment inside the tank and shields is on the order of  $\mu\text{K Hz}^{-1/2}$ , a stability that is comparable to that on the LISA spacecraft. Two NPRO lasers at 1064 nm are independently stabilized to these cavities using a modulation-demodulation technique known as Pound-Drever-Hall (PDH) locking [4]. The beat between the two independently stabilized lasers is measured with a frequency counter and recorded. The time series of the beat note at 128 MHz is shown in figure 1(a). The time series shows a slope of roughly  $1 \text{ Hz s}^{-1}$  which is similar to the drifts expected in the Doppler shifts of the LISA spacecraft. Figure 1(b) shows the corresponding linear spectral density plotted along with the free-running noise and the LISA requirement. The design of the LISA lasers is still evolving but most designs assume a diode-pumped solid state laser very similar to our NPRO lasers as the front end of the LISA lasers. The laser frequency noise of our NPRO lasers meets the LISA requirements at almost all frequencies and provides realistic, LISA-like laser frequency noise for our LISA benchtop experiment.

### 2.2. Electronic phase delay

In LISA, one laser field travels 16 s from one spacecraft to the other before it is superimposed with the local laser. The beat signal between these two fields on all the spacecraft composes the main LISA signals. We have developed an electronic phase delay (EPD) technique to simulate the light travel time between the spacecraft [5]. Our technique utilizes a frequency-stabilized

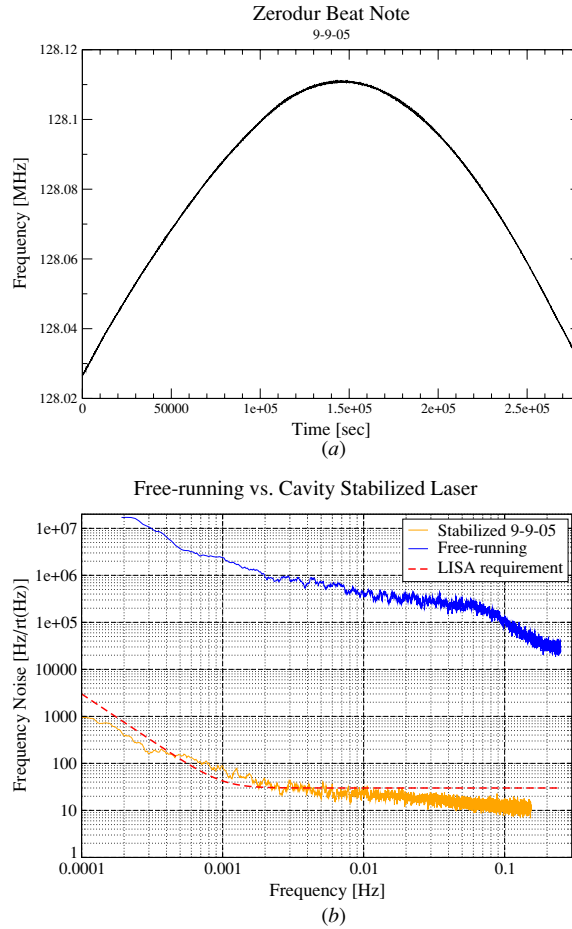


**Figure 1.** (a) Time series of the beat note frequency between the two independently stabilized lasers. (b) Frequency-stabilization results plotted along with the free-running noise and the LISA pre-stabilization requirement.

laser as a reference for all laser fields to be delayed. First, we detect the beat signal between the reference laser and the laser we want to delay. This beat signal will be digitized, stored in a memory buffer for a specified amount of time and then regenerated. The laser which represents the local laser in LISA is also superimposed with the reference laser. This prompt beat signal is then mixed with the delayed beat signal described above from the EPD unit. The resulting signal between a prompt-reference beat and delayed-reference beat is virtually identical to one of the main LISA signals; it has the same noise characteristics and dynamic properties, and can be used to test TDI and arm-locking with the correct LISA-like timescales.

**2.2.1. Electronic arm-locking.** A first generation of our EPD unit could digitize signals up to 30 kHz and could delay up to two signals by 80 s. At the time when the first EPD unit was completed, the laser stabilization was still under final development and we used a voltage-controlled oscillator (VCO) and an analogue phasemeter to perform our first arm-locking experiments [6]. Figure 2(a) shows the basic setup. The VCO signal is split; one part is digitized and delayed by 0.5 s with the EPD unit. The regenerated signal is mixed with the

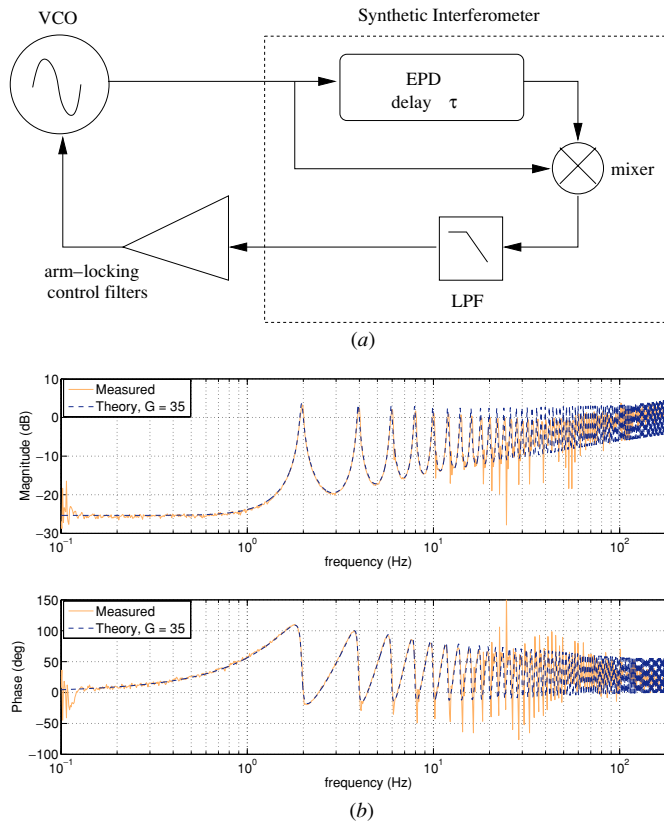


**Figure 2.** (a) Schematic diagram of how the EPD unit is used to create an interferometry signal for arm-locking. (b) Results of the electronic arm-locking experiment using the original delay unit with  $\tau = 0.5$  s. Details are discussed in [6].

instantaneous VCO signal, filtered, and this demodulated signal is the input to the arm-locking controller which stabilizes the VCO frequency to the delay. The resulting phase noise is shown in figure 2(b) and shows a good agreement with the predicted results. As shown in the plot, arm-locking provides good noise suppression at most frequencies except that there is actually slight noise enhancement at frequencies just below multiples of the inverse round-trip time, crossing through 0 dB at  $n/\tau$ ,  $n \in 1, 2, 3, \dots$

We have recently increased the bandwidth of the EPD unit using a faster ADC to be able to delay signals up to 5 MHz for as much as 6 s. This improved EPD unit was used to perform the first TDI experiments discussed in section 3.1. A future and final iteration will allow us to digitize signals as high as 25 MHz for more than 33 s to include the full LISA round-trip time. By using the benchtop simulator to supply the optical signals and using the final version of the EPD unit and real-time phasemeter, we will perform further studies of arm-locking with frequency-stabilized lasers instead of low-noise VCOs.

### 2.3. Phasemeter

The key hardware component in LISA is the phasemeter, which must measure the phase of a laser beat signal at 5–20 MHz with at least  $10^{-5}$  cycles  $\text{Hz}^{-1/2}$  accuracy. The LISA phasemeter

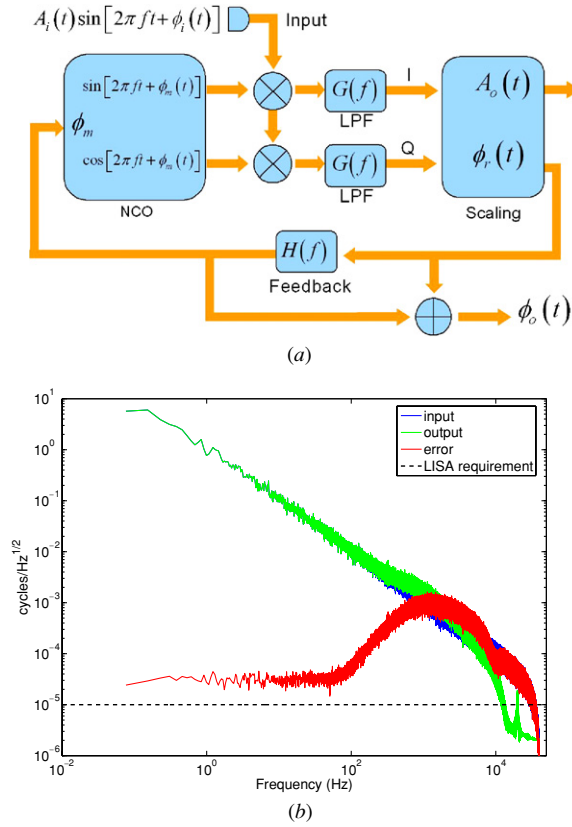


**Figure 3.** (a) Phasemeter schematic diagram. NCO stands for a numerically controlled oscillator and LPF stands for a low-pass filter. (b) Plot of a known input phase, the output phase computed with the Simulink phasemeter and the difference between the two.

is currently under development at the Jet Propulsion Laboratory. The design is based on an IQ demodulation phasemeter with a tracking numerically controlled oscillator (NCO) to avoid problems with wrapping [7]. Figure 3 shows the concept behind the design. The input signal at frequency  $f$  and phase  $\phi_i(t)$  is multiplied by the sine and cosine generated by an NCO with frequency  $f$  and phase  $\phi_m(t)$ . The multiplied signals are low-pass filtered to remove the second harmonic and give the in-phase and quadrature components which are then used to compute the amplitude and residual phase. The residual phase,  $\phi_r(t)$ , is the difference between  $\phi_i(t)$  and  $\phi_m(t)$  and is fed back to the NCO to adjust  $\phi_m(t)$ . As long as the feedback gains  $H(f)$  are appropriate, the model phase will stay close to the input phase and  $\phi_r(t) < 1$  cycle. By adding the residual phase to the model phase, we get the output phase  $\phi_o(t)$ .

The first iteration of the phasemeter is run off-line in Matlab's Simulink. It is designed for 10 kHz signals sampled at 80 kHz, set by the sampling frequency of the data acquisition hardware. The large data rates limit our experiments to roughly 2 min. Figure 3(b) shows the various phases computed by the phasemeter in a simulation for a known input signal. The input and output phases are roughly the same, both following the slope  $1/f$ . The error between the input phase and the output phase is reduced in noise. It is roughly  $6 \times 10^{-5}$  cycles/Hz<sup>1/2</sup> below 100 Hz, above which the filters in the phasemeter cause some of the phase information to be lost.

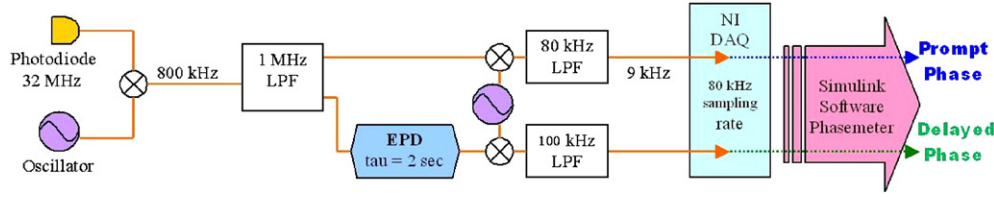


**Figure 4.** Schematic diagram of the initial optical experiment.

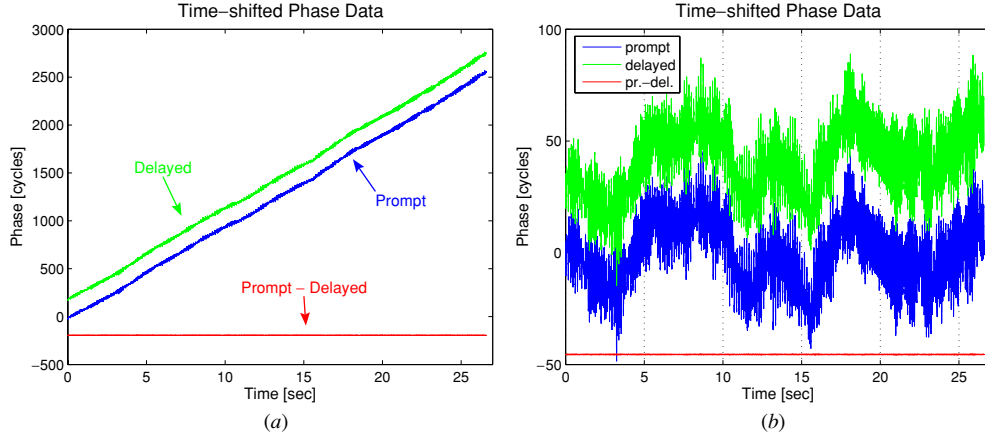


**Figure 5.** (a) The prompt phase after truncation,  $\phi_p(t)$ , time-shifted delayed phase,  $\phi_d(t - \tau_{\text{shift}})$ , and the time-delayed combination,  $S(t)$ , of these two signals. (b) Same phase signals as plot (a) but the linear slope has been removed from the prompt and delayed phase signals. The time-delayed combination is the same as in plot (a) and is computed from the non-detrended signals. A vertical offset has been applied to the delayed and time-delayed combination phases for appearance in the graph.

### 3. Applications of simulator

#### 3.1. Initial optical experiment

TDI relies upon combining time-shifted versions of the interferometry signals. Hence, our first experiments looked at just recombining a delayed signal shifted back in time with its prompt counterpart. This experiment not only provides a test of the TDI concept but also a system level test of the optical and electronic components of the benchtop simulator. The beat note between the two cavity-stabilized lasers was reduced by changing the laser frequencies by a few spectral ranges of their respective cavities. Referring to the experimental schematic diagram of figure 4, the beat note now at 32 MHz was mixed to a lower frequency of roughly 800 kHz and electronically split. The delayed signal is formed by putting one of these signals through the improved EPD unit with a delay of 2 s. Then, both signals are again mixed to a lower frequency of roughly 9 kHz to be recorded on a National Instruments DAQ at an 80 kHz sampling rate. The two function generators (or oscillators) and the EPD unit have their time bases linked to a common rubidium standard. After recording these voltage signals, they are run off-line through the Simulink software phasemeter to give the phases of the prompt and delayed signals,  $\phi_p(t)$  and  $\phi_d(t)$ , respectively. Figure 5 shows the phase signals. The slope of the signals in figure 5(a) is an inconsequential constant due to the difference between the signal

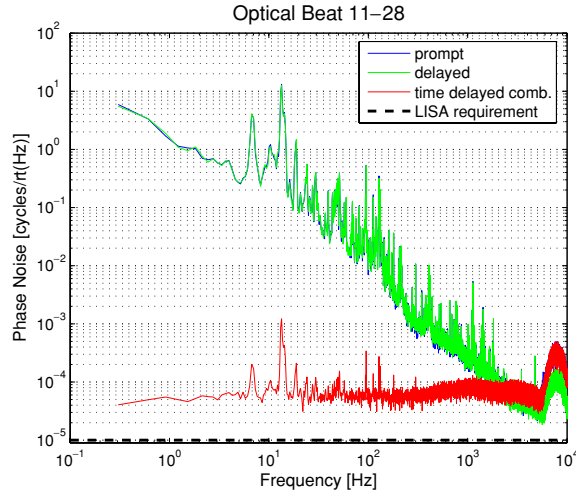


**Figure 6.** Linear spectral noise densities of the prompt, delayed and time-delayed combination phase signals.

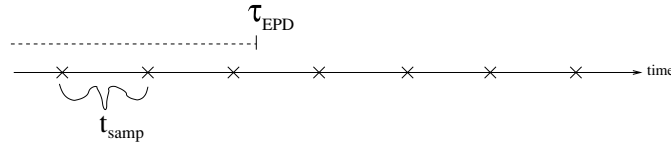


**Figure 7.** Schematic representation of timing in the experiment. The x's represent when the signals are sampled by the ADC where  $t_{\text{samp}} = 1/f_{\text{samp}}$ .

frequency and initial model frequency used for the NCO in the phasemeter. To compute the TDI-like combination, the first 2 s of the delayed phase data are removed, yielding  $\phi_d(t - \tau_{\text{shift}})$  where  $\tau_{\text{shift}}$  is the post-process shift imposed on the data set. Likewise, the last 2 s of the prompt phase data are removed so that the data sets are of the same length. It is these two truncated phase signals that are shown in figure 5(a). In order to see the structure in the phase signals more clearly, the linear slope has been removed from  $\phi_p(t)$  and  $\phi_d(t - \tau_{\text{shift}})$  in figure 5(a) and plotted in figure 5(b). The time-delayed combination is then

$$S(t) = \phi_p(t) - \phi_d(t - \tau_{\text{shift}}). \quad (1)$$

This time-delayed combination is also plotted in figures 5(a) and (b). The combination  $S(t)$  has less noise than its constituent signals as shown in the time series and more clearly in the frequency domain as plotted in figure 6. At the lower frequencies of the experiment, there are over five orders of magnitude suppression of laser phase noise and the noise in the time-delayed combination signal is within a factor of 4 of meeting the LISA requirements.

**3.1.1. Suppression limit.** The noise suppression in our experiments is so far primarily limited by the timing resolution of the original data sets. Consider that the EPD unit will produce a signal with delay  $\tau_{\text{EPD}}$ , as shown in figure 7. Most likely this delay in the experiment will not fall exactly at one of the sampling points,  $nt_{\text{samp}}$ ,  $n \in 1, 2, 3, \dots$ , but rather somewhere in between. The maximum time that could be between  $\tau_{\text{EPD}}$  and one of the sampling points

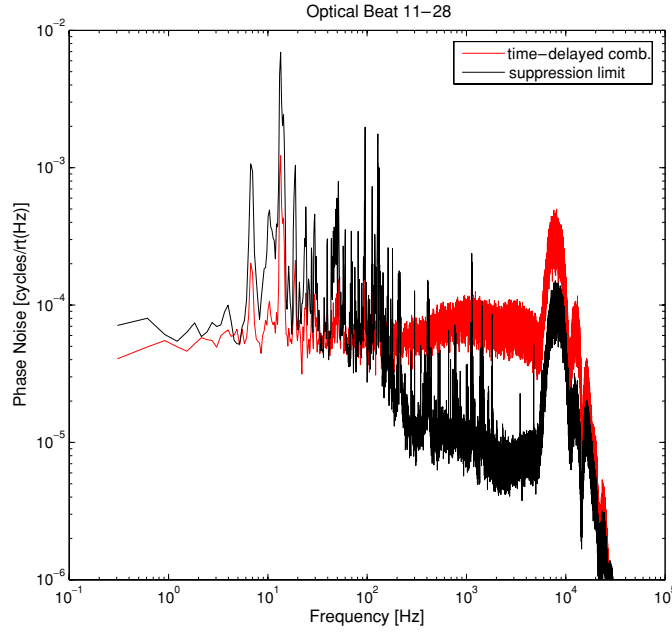


**Figure 8.** Linear spectral densities of the time-delayed combination and the worst-case timing suppression limit of  $\Delta\tau = \frac{1}{2}t_{\text{samp}} = 6.25 \mu\text{s}$ .

is  $\frac{1}{2}t_{\text{samp}}$ . Referring back to equation (1) and assuming  $\phi_d(t) = \phi_p(t + \tau_{\text{EPD}})$ , the time-delayed combination can be expressed as

$$S(t) = \phi_p(t) - \phi_p(t - \Delta\tau), \quad (2)$$

where  $\Delta\tau$  is the timing error:

$$\Delta\tau = |\tau_{\text{EPD}} - \tau_{\text{shift}}|. \quad (3)$$

We are interested in the noise of this signal in the frequency domain

$$\tilde{S}(f) = \int dt S(t) e^{-i2\pi ft} = \tilde{\phi}_p(f)[1 - e^{-i2\pi f \Delta\tau}], \quad (4)$$

and then computing the magnitude since we measure real signals yields

$$|\tilde{S}(f)| = 2 \sin(\pi f \Delta\tau) |\tilde{\phi}_p(f)|, \quad (5)$$

which gives a relation of the phase noise of the time-delayed combination to the phase noise of its constituent signals and the timing error.

Following equation (5), the worst-case timing suppression limit was computed using  $\Delta\tau = \frac{1}{2}t_{\text{samp}} = 6.25 \mu\text{s}$  and the measured phase noise of the prompt signal for  $|\tilde{\phi}_p(f)|$ . This suppression limit is plotted along with the linear spectral density of the time-delayed combination signal in figure 8. Above 100 Hz, the filters in the phasemeter affect the signal and some of the phase information is lost. Looking below 100 Hz, the spectrum of the time-delayed combination is slightly below the worst-case suppression limit due to the timing resolution. Therefore,  $\tau_{\text{EPD}}$  is closer to a sampling point than the maximum timing error of  $\frac{1}{2}t_{\text{samp}}$ , and our timing error is less than  $6.25 \mu\text{s}$ . We are currently investigating interpolation techniques which will allow us to reduce the data sets significantly and test methods that will be used on the LISA data streams [8].



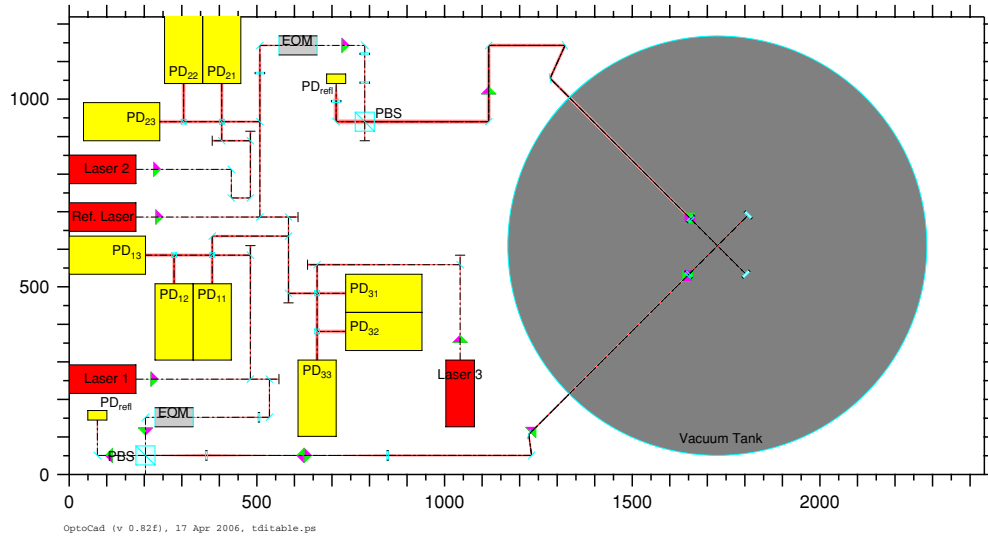


**Figure 9.** OptoCad layout of the benchtop simulator on a standard  $4 \times 8$  ft optical table. The axes are labelled in millimetres. Each laser beats with the reference laser at three photodiodes (PDs). The reference laser and laser 1 are frequency stabilized to the reference cavities. EOM stands for the electro-optic modulator and PBS stands for the polarizing beam splitter.

### 3.2. Applications of optical layout

Our benchtop simulator consists of four lasers: one representing each spacecraft plus a reference laser used to beat all the lasers into the RF band for detection. By taking each laser beat note and measuring it, or delaying and measuring it, we can recreate all signals used in LISA interferometry. The benchtop simulator resides on a standard  $4 \times 8$  ft optical table, as shown in figure 9. Roughly, half of the table supports the vacuum tank with thermal shields and reference cavities. The other half has the lasers and photodiodes as well as the associated optics for PDH locking. In the current iteration of the simulator, all beat signals between the lasers are taken from the same beam splitter which means that in first order we are insensitive to optical path length changes.

### 3.3. Future additions to simulator

By splitting the optical paths of the beams in the simulator, we can recreate several additional aspects of LISA. Passing one of the beams through an acousto-optic modulator will give the frequency shift similar to the Doppler shifts that will be experienced by LISA. We can also broaden the TDI experiments to include second-generation algorithms which have terms to account for the spacecraft motion [9]. We will also put a mirror on a PZT and inject gravitational wave signals. With such an ability, the signals from our benchtop simulator can be used as a testbed for data analysis algorithms and mock data challenges.

## 4. Conclusion

The LISA benchtop simulator at UF provides a solid testing ground for LISA interferometry. The pre-stabilized lasers provide realistic LISA-like laser phase noise to our optical

interferometry signals which are delayed on LISA timescales via the EPD unit and read with a LISA-like phasemeter. Current results include electronic arm-locking and a first optical test of the TDI concept. The current benchtop simulator also allows us to begin investigating issues with data reduction techniques, interpolation and how the data will be packaged for transmission from the spacecraft to earth. The next generation of improvements to the simulator will include Doppler shifts and injected gravitational wave signals which will provide highly realistic data streams for analysis tests.

### Acknowledgments

The authors wish to acknowledge Paul McNamara and Jeff Livas for useful discussions as well as Daniel Shaddock and Brent Ware for dialogue concerning the phasemeter. The authors would also like to thank Roland Schilling for use of his program OptoCad. This research was supported by the NASA/OSS grants BEFS04-0019-0019 and APRA04-0095-0007. Rachel Cruz thanks the NASA Harriet G Jenkins Predoctoral Fellowship Program for support.

### References

- [1] Bender P *et al* 1998 LISA Pre-Phase A Report 2nd edn *Max-Planck-Institut für Quantenoptik Technical Report* MPQ 233
- [2] Sheard B S, Gray M B, McClelland D E and Shaddock D A 2003 Laser frequency stabilization by locking to a LISA arm *Phys. Lett. A* **320** 9
- [3] Armstrong J W, Estabrook F B and Tinto M 1999 Time-delay interferometry for space-based gravitational wave searches *Astrophys. J.* **527** 814
- [4] Drever R W P, Hall J L, Kowalski F V, Hough J, Ford G M, Munley A J and Ward H 1983 Laser phase and frequency stabilization using an optical resonator *Appl. Phys. B* **31** 97
- [5] Thorpe J I, Cruz R J, Sankar S and Mueller G 2005 Electronic phase delay—a first step towards a bench-top model of LISA *Class. Quantum Grav.* **22** S227
- [6] Thorpe J I and Mueller G 2005 Experimental verification of arm-locking for LISA using electronic phase delay *Phys. Lett. A* **342** 199
- [7] Shaddock D A and Ware B 2005–2006 personal correspondence *NASA JPL*
- [8] Shaddock D A, Ware B, Spero R E and Vallisneri M 2004 Post-processed time-delay interferometry for LISA *Phys. Rev. D* **70** 081101
- [9] Shaddock D A, Tinto M, Estabrook F B and Armstrong J W 2003 Data combinations accounting for LISA spacecraft motion *Phys. Rev. D* **68** 061303